International Journal of Computational and Experimental Science and ENgineering (IJCESEN)

Vol. 10-No.4 (2024) pp. 549-559
http://www.ijcesen.com

ISSN: 2149-9144

Research Article

Radiation Shielding Characteristics and Transmission Factor values of some Selected Alloys: A Monte Carlo-Based Study

Duygu SEN BAYKAL[1], Ghada ALMISNED [2], Hessa ALKARRANI [3,4], H.O. TEKIN [5,6,7*]

[1] Istanbul Nisantasi University, Faculty of Engineering and Architecture, Mechatronics Engineering, 34398, Istanbul, Türkiye
Email: duygu.senbaykal@nisantasi.edu.tr - **ORCID:** 0000-0001-9833-9392

[2] Department of Physics, College of Science, Princess Nourah Bint Abdulrahman University, P.O. Box 84428, Riyadh, 11671, Saudi Arabia
Email: gaalmisned@pnu.edu.sa - **ORCID:** 0000-0001-9072-4480

[3] Research Institute for Medical and Health Sciences, University of Sharjah, Sharjah, 27272, Sharjah, United Arab Emirates
[4] Department of Medical Diagnostic Imaging, College of Health Sciences, University of Sharjah, 27272, Sharjah, United Arab Emirates
Email: halkarrani@sharjah.ac.ae - **ORCID:** 0009-0001-7823-5892

[5] Department of Medical Diagnostic Imaging, College of Health Sciences, University of Sharjah, 27272, Sharjah, United Arab Emirates
[6] Istinye University, Faculty of Engineering and Natural Sciences, Computer Engineering Department, Istanbul 34396, Türkiye
[7] Department of Physics and Technical Sciences, Western Caspian University, Baku, Azarbaijan
***Corresponding Author Email:** htekin@sharjah.ac.ae - **ORCID:** 0000-0002-0997-3488

Article Info:

DOI: 10.22399/ijcesen.421
Received : 16 August 2024
Accepted : 02 October 2024

Keywords :

Radiation Shielding
Alloy Composition
Phy-X/PSD
MCNP

Abstract:

Protecting the safety of both human health and the environment necessitates the careful management of radiation. Hence, it is important to possess effective radiation shielding since unregulated exposure to radiation may lead to significant health risks and environmental damage. Utilizing appropriate materials with strong radiation shielding characteristics is a crucial element of this safeguarding. This research examines the efficacy of eight different alloy types in attenuating radiation. The materials listed include 304 stainless steel, Inconel 718, Hastelloy C-276, Alloy 600, Nickel 200, D9 alloy, Maraging Steel 250, and Nimonic 80A. Each alloy has distinct mechanical qualities and exhibits exceptional resistance to corrosion, making them very useful and versatile in many applications. The research used Phys-X/PSD software and MCNP Monte Carlo simulations to assess the effectiveness of these alloy types as shielding agents. Considering the superior resistance of Hastelloy C-276 to gamma radiation, it is evident that this material has the capacity to be an exceptional option for shielding against radiation.

1. Introduction

Radiation plays a critical role in a wide range of applications, such as energy production and medical practices. In particular, radiation control has paved the way for technological advancements in fields like nuclear energy, medical imaging, and radiotherapy [1]. However, to prevent potential hazards to human and environmental health, it is essential to manage radiation safely. Uncontrolled radiation exposure can lead to serious health and environmental threats, making effective radiation protection of paramount importance [2]. Radiation shielding parameters determine how effectively the materials used can protect against radiation, and correctly determining these parameters is crucial for safe shield design [3]. Different materials offer various properties for radiation shielding. For instance, 304 Stainless Steel provides high corrosion resistance and mechanical durability due to its chromium and nickel content. Inconel 718 is a super-nickel alloy that exhibits superior mechanical

properties at high temperatures. Hastelloy C-276, widely used in the chemical processing industry, is resistant to corrosion across a wide temperature range due to its nickel, molybdenum, and chromium composition. On the other hand, Alloy 600, a nickel-chromium alloy, is preferred for high-temperature applications, especially in nuclear reactor components [4-8]. Nickel 200, composed almost entirely of pure nickel, offers high thermal and electrical conductivity. D9 Alloy, an iron-nickel-based alloy, is used as a structural material in nuclear reactors, providing high-temperature resistance and a low thermal stress coefficient. Maraging Steel 250 is a high-strength steel alloy resistant to oxidation and corrosion at high temperatures. Nimonic 80A, a nickel-chromium-based superalloy, is used in applications requiring high temperatures [9-11]. These alloys are widely used in critical industries such as nuclear energy, aerospace, medical imaging, radiotherapy, chemical processing, and military defense systems, where their radiation shielding capabilities, high-temperature resistance, and mechanical durability are essential.

2. Material and Methods

This study examines the radiation shielding capacities by using the Phys-X/PSD program [12] and MCNP Monte Carlo simulations of the eight alloys mentioned above and emphasizes the importance of assessing these capacities safely and effectively. The alloys examined in this study are listed below;

- 304 Stainless Steel: 0.00081C+0.01009Si+0.00045P+0.00030S+0.18153Cr+0.02017Mn+0.70597Fe+0.08068Ni
- Inconel 718: 0.00097C+0.00604Al+0.00423Si+0.00018P+0.00018S+0.01208Ti+0.22944Cr+0.00423Mn+0.01208Co+0.63398Ni+0.06038Nb+0.03623Mo
- Hastelloy C-276: 0.00010C+0.00080Si+0.00040P+0.00030S+0.15500Cr+0.01000Mn+0.05500Fe+0.02000Co+0.55840Ni+0.16000Mo+0.04000W
- Alloy 600: 0.00152C+0.00507Si+0.00015S+0.16723Cr+0.01014Mn+0.08108Fe+0.72974Ni+0.00507Cu
- Nickel 200: 0.00015C+0.00100Si+0.00010S+0.00350Mn+0.00400Fe+0.99025Ni+0.00100Cu
- D9 Alloy: 0.00150C+0.00500Si+0.00040P+0.00030S+0.12000Cr+0.02000Mn+0.73280Fe+0.12000Ni
- Maraging Steel 250: 0.00010Al+0.00301Ti+0.67628Fe+0.09017Co+0.18034Ni+0.05010Mo
- Nimonic 80A: 0.00010B+0.00100C+0.01500Al+0.01000Si+0.02200Ti+0.20000Cr+0.01000Mn+0.72090Fe+0.02000Co+0.00100Cu

2.1 Shielding Parameters

2.1.1. Linear Attenuation Coefficient

The relationship between the number of attenuated gamma rays I(x) and the number of unattenuated gamma rays $I_0(x)$ passing through a material of thickness (x) is defined in the area of radiation experimental study.

$$I(x) = I_0 e^{-\mu x} \quad (1)$$

The symbol μ represents the likelihood of complete contact per unit thickness in a shield material, and is referred to as the linear attenuation coefficient, measured in cm^{-1}.

2.1.2. Mass Attenuation Coefficient

The mass attenuation coefficient ($\mu_m = \mu/\rho$) is essential in calculating the linear attenuation coefficient for different materials. It is often used in many disciplines, such as medical imaging, to evaluate the radiation absorption characteristics of different substances [13-15].

2.1.3. Half-Value Layer

The half-value layer (HVL) is the minimum thickness of a substance needed to lower the intensity of radiation by 50%. The calculation is performed using the formula:

$$HVL = \frac{ln(2)}{\mu} \quad (2)$$

μ is the linear attenuation coefficient of the material. HVL, or half-value layer, is a crucial parameter used to evaluate the efficiency of materials in shielding against radiation [13-15].

2.1.4. Tenth-Value Layer

The tenth-value layer (TVL) is the minimum thickness of a material required to reduce the number of photons by one-tenth [13-15].

$$TVL = \frac{ln(10)}{\mu} \quad (3)$$

2.1.5. Mean Free Path

The mean free path (MFP) is the average distance that a particle travels before it collides with other particles inside a substance. The calculation is performed using the accompanying formula:

$$mfp = 1/\mu \quad (4)$$

The symbol μ denotes the linear attenuation coefficient of the material. The mfp, or mean free path, is crucial for assessing the effectiveness of a material in decelerating or halting particles [13-15].

2.1.6. Effective Atomic Number

In composite materials, the Compton scattering interaction has an effect on the effective atomic number (Z_{eff}), which can be defined as the following formula:

$$Z_{eff} = \frac{\sigma_T}{\sigma_e} \quad (5)$$

where σ_T and σ_e are the total and electronic cross-sections, respectively [13-15].

2.1.7. Effective Electron Density

The effective electron density (N_{eff}) is a crucial quantity for comprehending the interaction between radiation and a substance. The electron density of the substance determines its dependency [13-15].

2.1.8. Fast neutron effective removal cross-section (Σ_R) values

The (Σ_R) is a crucial quantity in the area of nuclear shielding, particularly in sites where there is a considerable danger of neutron exposure. The value of Σ_R varies inversely with the mean free path of neutrons in the material. For instance, a high Σ_R value indicates that the material has a greater ability to efficiently reduce the intensity of fast neutrons [16]. This research analyzed all radiation shielding factors using the Phy-X/PSD program, which allows for exact simulations of various alloy compositions and thicknesses.

2.2 MCNP Monte Carlo Simulations for Transmission Factor (TF) Calculations

The Monte Carlo method is a fundamental approach in radiation physics that enables the modeling and analysis of intricate systems via the use of random sampling methods [16]. The adaptability of this technique is especially apparent in the assessment and enhancement of radiation shielding, where accurate simulation of particle interactions with materials is essential. The Monte Carlo approach essentially simulates the movement and interaction of individual particles, such as electrons, photons, and neutrons, as they travel through and interact with various substances [17]. This technique produces statistical data by modeling the trajectories of many particles, providing significant insights into the effectiveness of a material in blocking or lowering radiation [18]. The Monte Carlo approach is advantageous because it can faithfully reproduce the complicated behaviors of particles as they experience complex processes inside materials. Accurate identification of the simulation geometry is essential for the efficiency of a Monte Carlo simulation. This geometry encompasses the spatial configuration of the radiation source, shielding material, and detector sections in the simulation. Within a simplified planar shield model, the geometry encompasses the dimensions, composition, and spatial configuration of the shielding material in relation to the radiation source and detectors [19]. Precision in geometry is crucial since even minor inaccuracies in its specification may have significant repercussions on the reliability of simulations, hence compromising the capacity to draw valid conclusions about the material's protective capabilities. To guarantee the precision of the simulation, it is crucial to show prudence while describing the density, atomic number, and dimensions of the material. The F4 tally mesh is an essential tool for assessing the outcomes of Monte Carlo simulations [20].

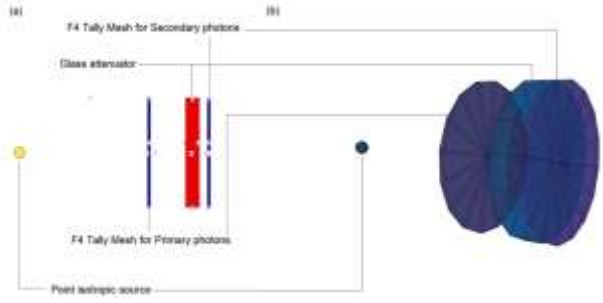

Figure 1. *(a) 2-D and (b) 3-D illustrations of designed MCNP simulation setup.*

This mesh serves as a measuring instrument by computing the radiation flux inside specific volumes of the simulated material. Figure 1 show that 2-D and 3-D illustrations of designed MCNP simulation setup.

3. Results and Discussions

A comprehensive analysis was conducted on eight distinct alloy samples to ascertain their fundamental shielding properties against gamma rays within the energy range of 0.015–15 MeV. The gamma ray shielding ability of a material is intimately correlated to its density and atomic structure, which are well recognized [21-25]. The density values of all the alloys under investigation are shown in Figure 2. We have identified a crucial parameters for gamma ray shielding, namely the linear attenuation coefficient (LAC) and mass attenuation coefficients (MAC). The LAC and MAC data demonstrate a decline as the gamma energy increases within the low energy range as seen in Figure 3. The Hastalloy C-276 alloy type had the highest LAC and MAC values at the photon energy we studied.

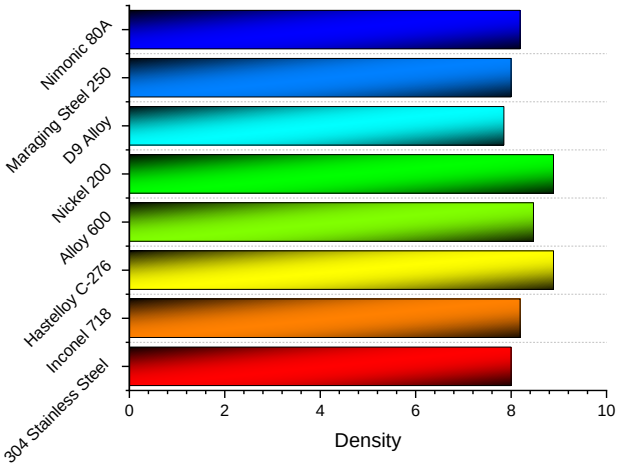

Figure 2. *Variation of investigated alloy types and densities.*

The alloy types under investigation are also evaluated in terms of their half-value layer (HVL). HVL is a critical parameter used to calculate the thickness of shielding material required to decrease the starting intensity by 50% [25-30]. Figure 4 depicts the variations in the HVL values of the alloy types in relation to the energy of the incoming photons. As the energy of the incoming photons rises, the HVL values of the alloy types also increase. However, the Hastalloy C-276 alloy type consistently exhibits the lowest HVL values across all energy levels. Based on the results of the tenth value layer (TVL) calculation, it is much easier to choose the right shielding material. This is especially important in nuclear radiation and medical diagnostics applications. Figure 4 depicts the energy-dependent fluctuation of one-tenth of the thickness of the investigated alloy types. It is clear that the TVL values have greater quantitative values than the HVL values for the identical energy values. Despite the fact that these two parameters had varying numerical values for identical energy levels, the research findings indicate that the Hastalloy C-276 alloy type exhibited the lowest values in thicknesses equivalent to one-tenth of the total thickness. Based on the findings derived from these two important properties, the Hastalloy C-276 alloy type will provide minimum thickness values that are half and one-tenth of the value in any process operating between the 0.015–15 MeV photon energy range. The mean free path (MFP) is a crucial determinant of a material's radiation shielding capabilities. Figure 5 depicts a visual depiction of the MFP values for eight different alloy types. The lowest measured MFP values for the Hastalloy C-276 alloy type are provided at different gamma ray energies. Accurately determining the effective removal cross-section values for fast neutrons is crucial for evaluating how well materials can protect against this kind of radiation. Materials with high effective removal cross-section values for fast neutrons may effectively attenuate or absorb a larger percentage of these particles, resulting in a reduced capacity for them to permeate through the material. Figure 6 displays the Effective Removal Cross Section (Σ_R, 1/cm) values for the investigated alloys being studied. Ninomic 80A have good neutron absorption properties. The effective atomic number (Z_{eff}) is a valuable parameter for assessing a material's appropriateness for gamma-ray applications, as it relates to the material's capacity to attenuate gamma rays and mitigate their effects [31-35].

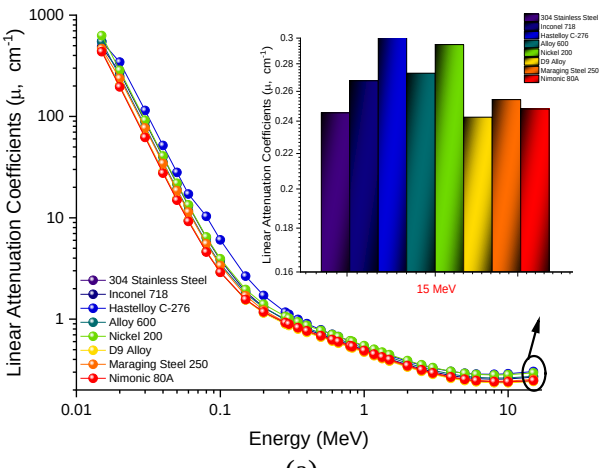

(a)

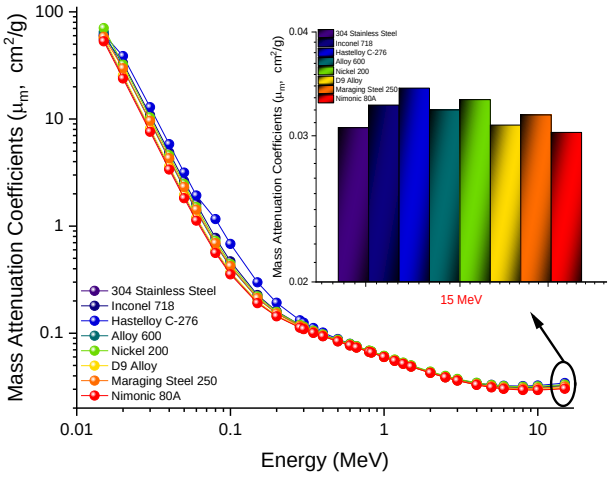

(b)

Figure 3(a-b). *Variation of linear attenuation coefficient (cm^{-1}) with photon energy (MeV) and mass attenuation coefficients (cm^2/g)for all investigated alloy types.*

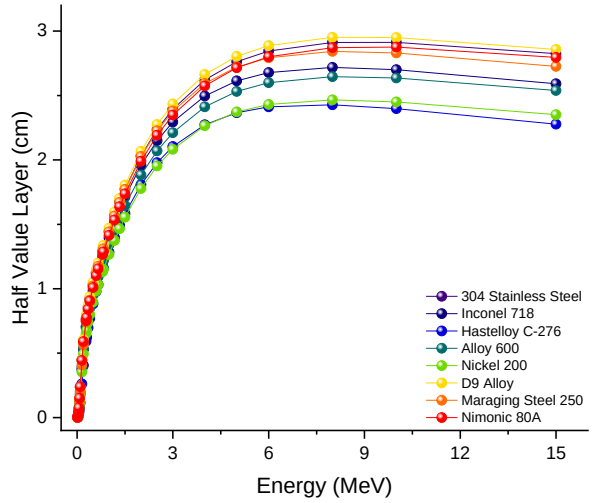

(a)

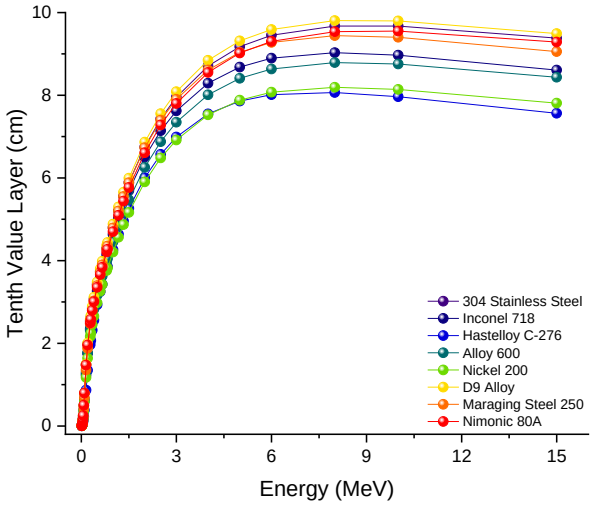

(b)

Figure 4. *Variation of the half-value layer (cm) and the tenth-value layer (cm) with photon energy (MeV) for all investigated alloy types.*

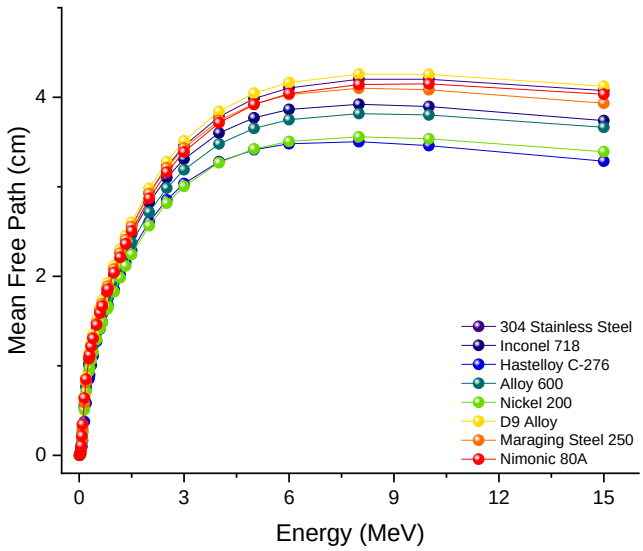

Figure 5. *Variation of mean free path (cm) with photon energy (MeV) for all investigated alloy types.*

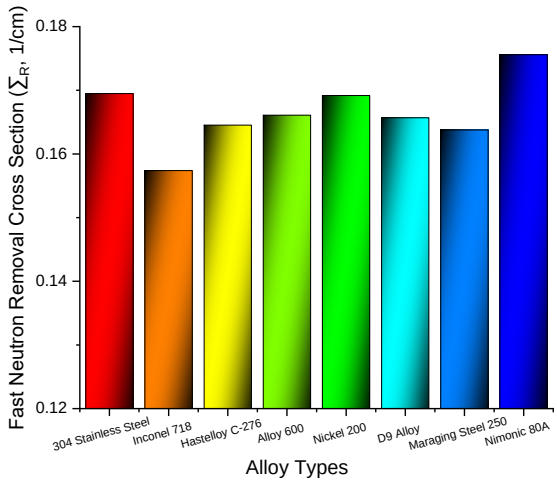

Figure 6. *Variation of fast neutron removal cross section ($\sum_R$, 1/cm) values of all investigated alloy types.*

Figure 7 displays the Z_{eff} values of the examined alloy types in relation to the energy of photons. The findings indicate that the Hastalloy C-276 alloy type has the highest Z_{eff} value. Figure 8 demonstrates a linear correlation between the effective atomic number (N_{eff}) and the N_{eff} values of Hastalloy C-276 alloy type. Figure 9 illustrates the relationship between energy and exposure buildup factor (EBF) for various mean free path (mfp) values. Various types of chemical reactions take place in a wide range of natural situations. There is a significant relationship between the binding energies of elements with high atomic numbers and their atomic numbers, leading to a distinct peak in the first area. The EBF values remain consistent inside the Compton resonance zone. Pair production is considered the third most important sector due to the fact that absorption processes

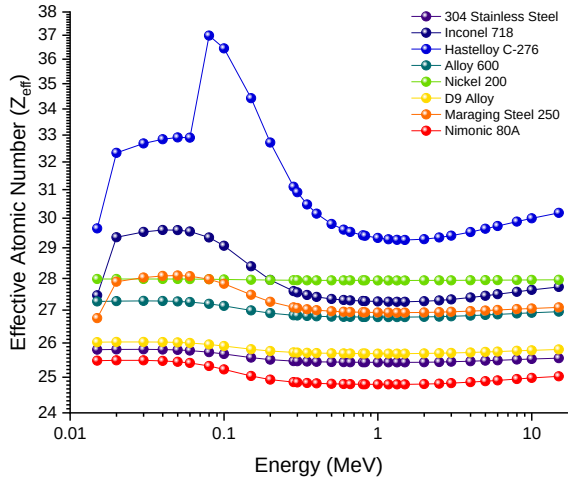

Figure 7. *Variation of effective atomic number (Z_{eff}) with photon energy (MeV) for all investigated alloy types.*

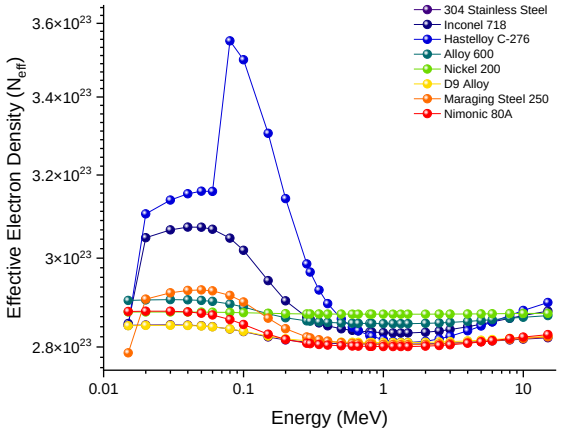

Figure 8. *Variation of effective electron density (N_{eff}, electrons/g) with photon energy (MeV) for all investigated alloy types.*

lead to a slight rise in EBF. The Hastalloy C-276 alloy type has the lowest identified EBF value. This illustrates the effectiveness of materials in reducing the effects of gamma radiation. The Hastalloy C-276 alloy demonstrated superior isolation compared to other investigated alloy types, which have the lowest EBF values. Figure 10 demonstrates a consistent relationship between the energy absorption building factor (EABF) and photon energy (MeV). The figure covers a range of 5 to 40 mean free paths (mfp). The MCNP technique was used in the last phase to compute the TF values for all the different alloy types. The MCNP method was used in the last step to calculate the transmission factor (TF) values for all kinds of alloys. The TF values of each alloy types were calculated by manipulating the energy levels and thicknesses. This method was used to examine the variations in thickness and energy of the alloy types being studied and how these affected

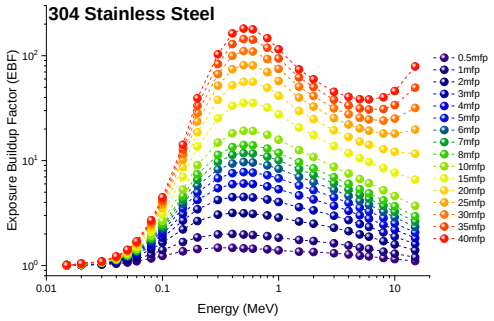

(a)

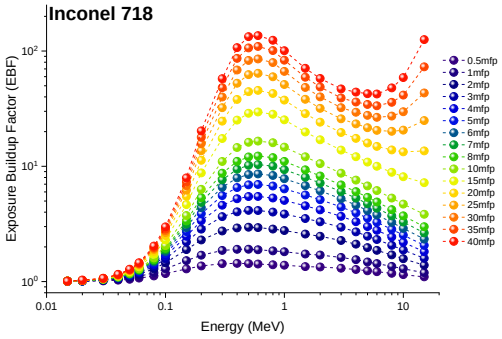

(b)

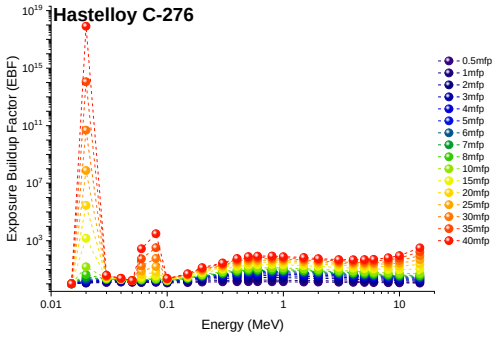

(c)

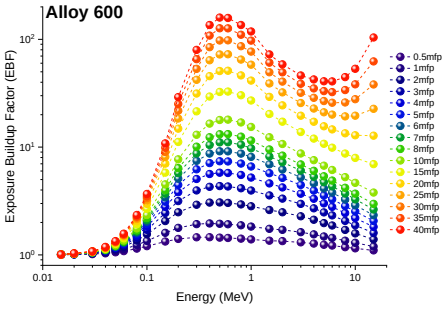

(d)

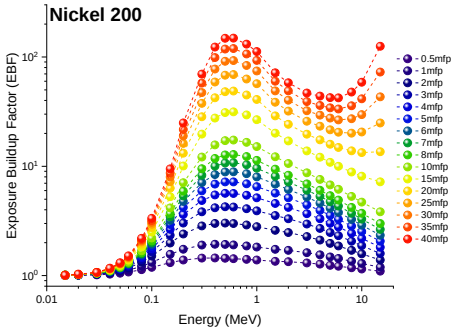

(e)

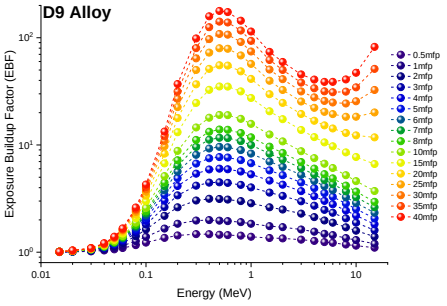

(f)

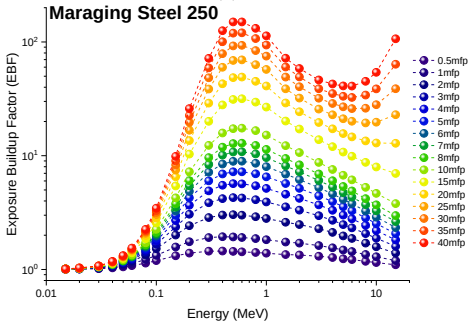

(g)

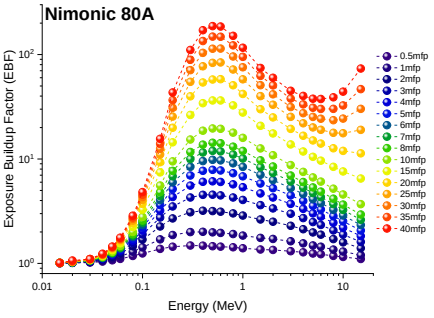

(h)

Figure 9(a-h). *Variation of exposure buildup factors (EBF) of all investigated alloy types at different mean free path values.*

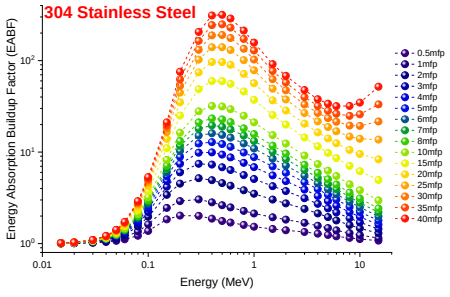

(a)

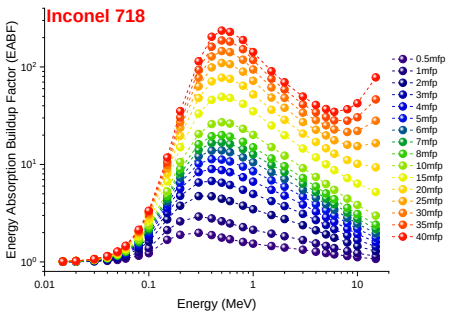

(b)

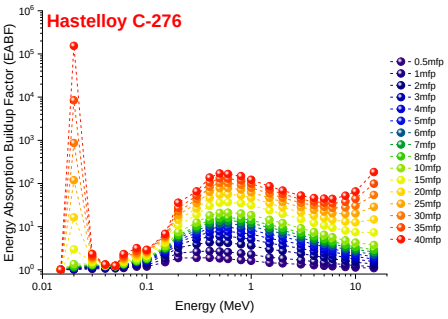

(c)

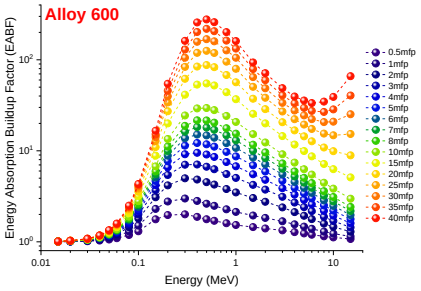

(d)

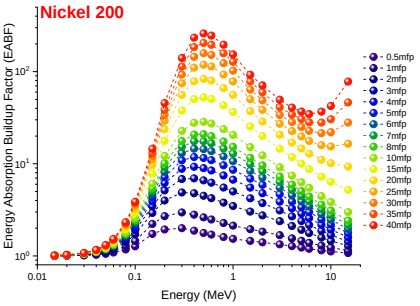

(e)

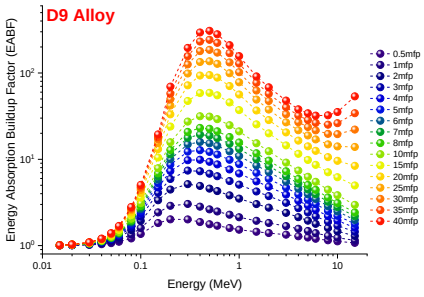

(f)

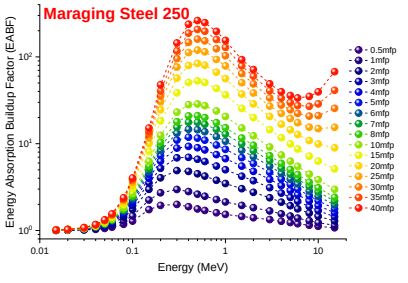

(g)

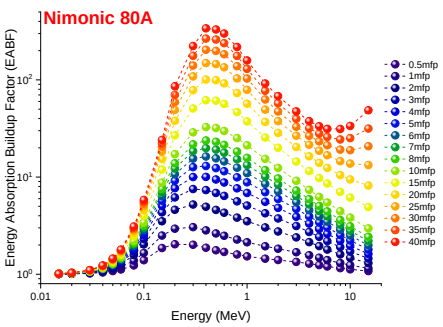

(h)

Figure 10(a-h). *Variation of energy absorption buildup factors (EABF) of all investigated alloy types at different mean free path values.*

the TF behaviors. Consequently, two F4 tally meshes yielded different results, which were later retrieved from the output file for the purpose of calculating transmission factors. After completing the input file, we executed the MCNP code using the specified input file as the selected input. Figure 11 illustrates the transmission factor (TF) values of the alloy types being studied. The graph illustrates an inverse relationship between TF values and alloy thickness, with a decreasing trend as the TF values grow. The behavior is consistent across different energy levels and may be attributed to the proportionate increase in gamma-ray absorption in the alloy attenuator. This increase is directly related to the equivalent increase in the thickness of the material. The greater absorption found in the thicker alloy resulted in a reduction in the emission of secondary gamma rays from the alloy attenuator. When comparing this decrease with the main gamma-ray parameter, the decrease in transfer function (TF) values becomes evident. The TF values shown by the Hastalloy C-276 alloy type, however, were much greater than those of the other alloy types.

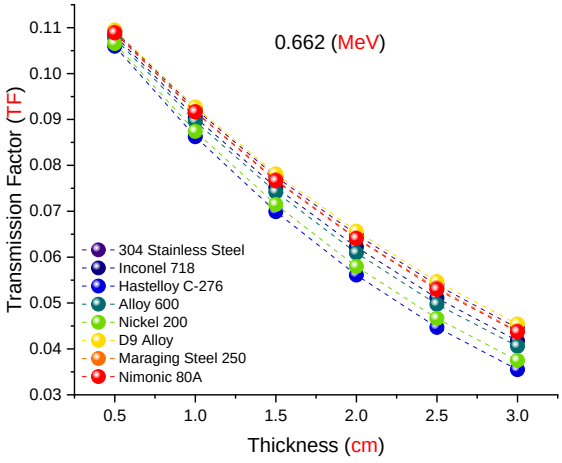

(a)

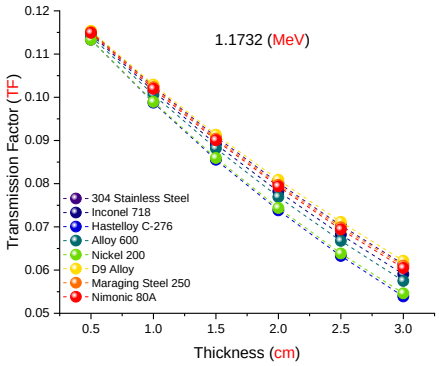

(b)

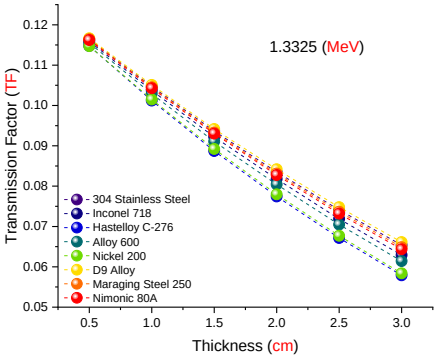

(c)

Figure 11(a-c). *Transmission Factors (TFs) of all investigated alloy types as a function of used radioisotope energy (MeV) at different alloy thicknesses.*

4. Conclusions

The study looks closely at how well eight different alloys attenuate the ionizing radiation, paying special attention to important numbers like the effective atomic number (Z_{eff}), the linear attenuation coefficient (LAC) and the mass attenuation coefficient (MAC). The study also looks at the half-value layer (HVL) and the tenth-value layer (TVL), as well as the mean free path (MFP) and the effective removal cross-section for fast neutrons (FNRCS). The findings consistently demonstrate that Hastelloy C-276 is the optimal material in many domains, making it an excellent selection for rigorous radiation shielding applications. Hastelloy C-276 had the greatest linear attenuation coefficient (LAC) and mass attenuation coefficient (MAC) values among the measured photon energies. This demonstrates its exceptional ability to effectively block gamma radiation. This alloy also exhibited the lowest half-value layer (HVL) and tenth-value layer (TVL) values, which are crucial for reducing the required thickness of shielding materials. Moreover, the low mean free path of Hastelloy C-276 renders it very effective in obstructing gamma rays. This is further

enhanced by its elevated effective atomic number, which enhances its total shielding capabilities. Additionally, the Effective Removal Cross Section (Σ_R) values identified in the study demonstrate Hastelloy C-276's superior protection against fast neutrons. The research further discovered that Hastelloy C-276 had the lowest EBF values, hence confirming its ability to efficiently reduce gamma radiation exposure. Furthermore, Hastelloy C-276 exhibited low Exposure Buildup Factor (EBF) values, underscoring its effectiveness in mitigating the adverse effects of gamma radiation. An important component of the research was analyzing the Fast Neutron Removal Cross Section (FNRCS), which is a crucial measure for evaluating a material's capacity to protect against fast neutrons, known for their challenging attenuation. Hastelloy C-276 and Nimonic 80A had better neutron absorption properties, which suggests they might work well in situations where protection against both gamma radiation and neutrons is needed. Furthermore, Monte Carlo simulations using the MCNP algorithm proved that Hastelloy C-276 had higher transmission factor (TF) values than the other alloys. As a result, it exhibited enhanced absorption characteristics and reduced secondary gamma ray emission. The Monte Carlo N-Particle (MCNP) simulations, which calculated Transmission Factor (TF) values at different energy levels and alloy thicknesses, revealed that Hastelloy C-276 displayed higher TF values compared to other alloy types. While these higher TF values indicate that more gamma radiation passes through this alloy, the proportion of absorbed radiation increased significantly when thicker alloy materials were used. The simulation results demonstrated a noticeable decrease in TF values as the alloy thickness increased, indicating enhanced gamma-ray absorption. Particularly at high energy levels of 15 MeV, Hastelloy C-276 maintained minimal TF values, providing excellent shielding. This reduction in TF values also implies a lower emission of secondary gamma rays. This thorough assessment highlights the crucial significance of choosing suitable materials for radiation shielding, especially in high-risk settings such as nuclear reactors and medical institutions. The results support the conclusion that Hastelloy C-276 is a great choice for radiation shielding because it protects well with a relatively thin material. To summarize, this study emphasizes the importance of choosing the right materials for radiation protection and emphasizes the ongoing need for research to create and enhance materials that can offer excellent shielding abilities while maintaining safety in different industrial and medical uses. The inclusion of FNRCS in the assessment process further exemplifies the need for a comprehensive approach to determining the most efficient shielding materials. For future research, it is recommended that the scientific community continues to explore the development of new alloy compositions and further investigates their radiation shielding properties, particularly in high-energy applications such as space exploration and advanced nuclear technologies.

Author Statements:

- **Ethical approval:** The conducted research is not related to either human or animal use.
- **Conflict of interest:** The authors declare that they have no known competing financial interests or personal relationships that could have appeared to influence the work reported in this paper
- **Acknowledgement:** The authors declare that they have nobody or no-company to acknowledge.
- **Author contributions:** The authors declare that they have equal right on this paper.
- **Funding information:** The authors declare that there is no funding to be acknowledged.
- **Data availability statement:** The data that support the findings of this study are available on request from the corresponding author. The data are not publicly available due to privacy or ethical restrictions.

References

[1] Singh, J., Singh, H., Sharma, J., Singh, T., & Singh, P. S. (2018). Fusible alloys: A potential candidate for gamma rays shield design. *Progress in Nuclear Energy*. 106;387-395 https://doi.org/10.1016/j.pnucene.2018.04.002

[2] Tekin, H. O., Kassab, L. R. P., Issa, S. A. M., Bordon, C. D. S., Altunsoy Guclu, E. E., da Silva Mattos, G. R., & Kilicoglu, O. (2019). Synthesis and nuclear radiation shielding characterization of newly developed germanium oxide and bismuth oxide glasses. *Ceramics International*, 45(18);24664-24674 https://doi.org/10.1016/j.ceramint.2019.08.204

[3] Abouhaswa, A. S., Tekin, H. O., Kavaz, E., & Perisanoglu, U. (2021). Optical and nuclear radiation protection characteristics of lithium bismo-borate glasses: Role of ZrO2 substitution. *Radiation Physics and Chemistry*. 183;109428 https://doi.org/10.1016/j.radphyschem.2021.109428

[4] Brookhaven National Laboratory. (n.d.). Materials handbook for fusion energy systems . Brookhaven National Laboratory.

[5] Special Metals Corporation. (n.d.). Inconel 718 technical data . Special Metals Corporation.

[6] Haynes International. (n.d.). Hastelloy C-276 technical data . Haynes International.

[7] Special Metals Corporation. (n.d.). Nickel 200/201 technical data . Special Metals Corporation.

[8] ASM International. (1990). ASM handbook, volume 2: Properties and selection: Nonferrous alloys and special-purpose materials . ASM International.

[9] ASM International. (1990). ASM handbook, volume 1: Properties and selection: Irons, steels, and high-performance alloys . ASM International.

[10] Special Metals Corporation. (n.d.). Inconel 600 technical data . Special Metals Corporation.

[11] Special Metals Corporation. (n.d.). Nimonic 80A technical data . Special Metals Corporation.

[12] Şakar, E., Özpolat, Ö. F., Alım, B., Sayyed, M. I., & Kurudirek, M. (2020). Phy-X / PSD: Development of a user-friendly online software for calculation of parameters relevant to radiation shielding and dosimetry. *Radiation Physics and Chemistry*, 166, 108496. https://doi.org/10.1016/j.radphyschem.2019.108496

[13] Kara, U., Kavaz, E., Issa, S. A. M., Rashad, M., Susoy, G., Mostafa, A. M. A., Yildiz Yorgun, N., & Tekin, H. O. (2020). Optical, structural, and nuclear radiation shielding properties of Li2B4O7 glasses: Effect of boron mineral additive. *Applied Physics A*, 126, 261. https://doi.org/10.1007/s00339-020-3397-8

[14] Tekin, H. O., Singh, V. P., & Manici, T. (2017). Effects of micro-sized and nano-sized WO3 on mass attenuation coefficients of concrete by using MCNPX code. *Applied Radiation and Isotopes*. 121;122-125 https://doi.org/10.1016/j.apradiso.2016.12.040

[15] Hosamani, M. M., & Badiger, N. M. (2018). Determination of effective atomic number of composite materials using backscattered gamma photons: A novel method. *Chemical Physics Letters.* 695;94-98 https://doi.org/10.1016/j.cplett.2018.02.012

[16] El-Khayatt, A. M. (2010). Calculation of fast neutron removal cross-sections for some compounds and materials. *Annals of Nuclear Energy*, 37(2), 218–222. https://doi.org/10.1016/j.anucene.2009.10.022

[17] Tekin, H. O., ALMisned, G., Issa, S. A. M., & Zakaly, H. M. H. (2022). A rapid and direct method for half-value layer calculations for nuclear safety studies using MCNPX Monte Carlo code. *Nuclear Engineering and Technology*. 54(9);3317-3323 https://doi.org/10.1016/j.net.2022.03.037

[18] ALMisned, G., Günoğlu, K., Varol Özkavak, H., Sen Baykal, D., Tekin, H. O., Karpuz, N., & Akkurt, I. (2023). An investigation on gamma-ray and neutron attenuation properties of multi-layered Al/B4C composite. *Materials Today Communications* . 36;106813 https://doi.org/10.1016/j.mtcomm.2023.106813

[19] Briesmeister, J. (2000). MCNP—a General Monte Carlo Code for Neutron and Photon Transport (Version 4C). National Laboratory, Los Alamos. Report LA-13709-M.

[20] ALMisned, G., Zakaly, H. M. H., Ali, F. T., Issa, S. A. M., Ene, A., Kilic, G., Ivanov, V., & Tekin, H. O. (2022). A closer look at the efficiency calibration of LaBr3(Ce) and NaI(Tl) scintillation detectors using MCNPX for various types of nuclear investigations. *Heliyon* , 10839. https://doi.org/10.1016/j.heliyon.2022.e10839

[21] Rammah, Y. S., Kumar, A., Mahmoud, K. A., El-Mallawany, R., El-Agawany, F. I., Susoy, G., & Tekin, H. O. (2020). SnO reinforced silicate glasses and utilization in gamma radiation shielding applications. *Emerging Materials Research*, 9(3). https://doi.org/10.1680/jemmr.20.00150

[22] Tekin, H. O., Abouhaswa, A. S., Kilicoglu, O., Issa, S. A. M., Akkurt, I., & Rammah, Y. (2020). Fabrication, physical characteristic, and gamma-photon attenuation parameters of newly developed molybdenum-reinforced bismuth borate glasses. *Physica Scripta* , 95, 115703. https://doi.org/10.1088/1402-4896/abbf6e

[23] Saddeek, Y. B., Issa, S. A. M., Altunsoy Guclu, E. E., Kilicoglu, O., Susoy, G., & Tekin, H. O. (2020). Alkaline phosphate glasses and synergistic impact of germanium oxide (GeO2) additive: Mechanical and nuclear radiation shielding behaviors. *Ceramics International*, 46(10);16781-16797 https://doi.org/10.1016/j.ceramint.2020.03.254

[24] Rammah, Y. S., Tekin, H. O., Sriwunkum, C., Olarinoye, I., Alalawi, A., Al-Buriahi, M. S., Nutaro, T., & Tonguc, B. T. (2020). Investigations on borate glasses within SBC-Bx system for gamma-ray shielding applications. *Nuclear Engineering and Technology* , 53, 282-293. https://doi.org/10.1016/j.net.2020.06.034

[25] Al-Buriahi, M. S., Arslan, H., Tekin, H. O., Singh, V. P., & Tonguc, B. (2020). MoO3-TeO2 glass system for gamma ray shielding applications. *Materials Research Express*, 7;025202 https://doi.org/10.1088/2053-1591/ab6db4

[26] Altunsoy, E. E., Tekin, H. O., & Mesbahi, A. (2020). MCNPX Simulation for Radiation Dose Absorption of Anatomical Regions and Some Organs. *Acta Physica Polonica A* , 137(4), 561-566. https://doi.org/10.12693/APhysPolA.137.561

[27] Abouhaswa, A. S., Zakaly, H. M. H., Issa, S. A. M., Rashad, M., Pyshkina, M., Tekin, H. O., El-Mallawany, R., & Mostafa, M. Y. A. (2021). Synthesis, physical, optical, mechanical, and radiation attenuation properties of TiO2–Na2O–Bi2O3–B2O3 glasses. *Ceramics International*, 47(1);185-204 https://doi.org/10.1016/j.ceramint.2020.08.122

[28] Kilic, G., Ilik, E., Issa, S. A. M., Issa, B., Al-Buriahi, M. S., Issever, U. G., Zakaly, H. M. H., & Tekin, H. O. (2021). Ytterbium (III) oxide reinforced novel TeO2-B2O3-V2O5 glass system: Synthesis and optical, structural, physical, and thermal properties. *Ceramics International*, 47(13);18517-18531 https://doi.org/10.1016/j.ceramint.2021.03.175

[29] Kavaz, E., Tekin, H. O., Kilic, G., & Susoy, G. (2020). Newly developed Zinc-Tellurite glass system: An experimental investigation on impact of Ta2O5 on nuclear radiation shielding ability. *Journal of Non-Crystalline Solids*, 544, 120169. https://doi.org/10.1016/j.jnoncrysol.2020.120169

[30] Kacal, M. R., Polat, H., Oltulu, M., Akman, F., Agar, O., & Tekin, H. O. (2020). Gamma shielding and compressive strength analyses of polyester composites reinforced with zinc: An experiment, theoretical, and simulation based study. *Applied Physics A*, 126, 205. https://doi.org/10.1007/s00339-020-3382-2

[31] Lakshminarayana, G., Kumar, A., Tekin, H. O., Issa, S. A. M., Al-Buriahi, M. S., Lee, D.-E., Yoon, J., & Park, T. (2020). Binary B2O3-Bi2O3 glasses: Scrutinization of directly and indirectly ionizing radiation shielding abilities. *Journal of Materials Research and Technology*, 14549-14567. https://doi.org/10.1016/j.jmrt.2020.10.019

[32] Abouhaswa, A. S., Rammah, Y. S., Sayyed, M. I., & Tekin, H. O. (2019). Synthesis, structure, optical, and gamma radiation shielding properties of B2O3-PbO2-Bi2O3 glasses. *Composites Part B: Engineering*, 172, https://doi.org/10.1016/j.compositesb.2019.05.040

[33] Kurtulus, R., Kavas, T., Akkurt, I., Günoğlu, K., Tekin, H. O., & Kurtulus, C. (2021). A comprehensive study on novel alumino-borosilicate glass reinforced with Bi2O3 for radiation shielding applications: Synthesis, spectrometer, XCOM, and MCNP-X works. *Journal of Materials Science: Materials in Electronics*, 32, 13882-13896. https://doi.org/10.1007/s10854-021-05964-w

[34] Al-Buriahi, M. S., Hegazy, H. H., Alrashedi, F., Olarinoye, I. O., Algarni, H., Tekin, H. O., & Saudi, H. A. (2021). Effect of CdO addition on photon, electron, and neutron attenuation properties of boro-tellurite glasses. *Ceramics International*, 47, 5951-5958. https://doi.org/10.1016/j.ceramint.2020.10.168

[35] Al-Buriahi, M. S., Alzahrani, J. S., Olarinoye, I. O., Akyildirim, H., Alomairy, S., Kebaili, I., Tekin, H. O., & Mutuwong, C. (2021). Role of heavy metal oxides on the radiation attenuation properties of newly developed TBBE-X glasses by computational methods. *Physica Scripta*, 96, 075302. https://doi.org/10.1088/1402-4896/abf86a